Chapter 3

Design of SIR Estimator

3.1 Introduction

Signal-to-interference ratio (SIR) estimator estimates the power ratio of the transmitted signal to the interference signal. Accurate measurement of SIR is required for the transmitted power control (TPC).

3.1.1 Conventional SIR Estimator

Conventional scheme, as shown in Figure 3.1, estimates the SIR by averaging the received pilot symbols over a fixed interval of one slot corresponding to 0.667 ms regardless of the channel condition, where the pilot symbols in the dedicated physical channel (DPCH) are used for the estimation of the channel condition. The instantaneous interference component can be obtained by removing the estimated signal from the received signal. The amount of the interference power is estimated by averaging the instantaneous interference over a few slots. Each finger of the rake receiver in the WCDMA system needs an SIR estimator. We assume that the multi-path channel has L resolvable paths and that there is no path loss and shadowing effect for ease of description. Since the SIR estimator is connected to the rake receiver, which has l fingers, of the mobile phone, therefore, the received signal of k^{th} slot from the l^{th} path of n^{th} symbol after despreading can be written as

$$r_l[n,k] = h_l[n,k]p[n,k] + z_l[n,k], \tag{3.1}$$

where n is the symbol sequence $\in \{0,1,...,7\}$, $h_l[n,k]$ is the complex channel gain (impulse response) of the n^{th} symbol in the k^{th} slot, $p[n,k]$ is the pilot sequence and $z_l[n,k]$ is the sum of the background noise and Multiple Access Interference (MAI) including the interference from other paths.

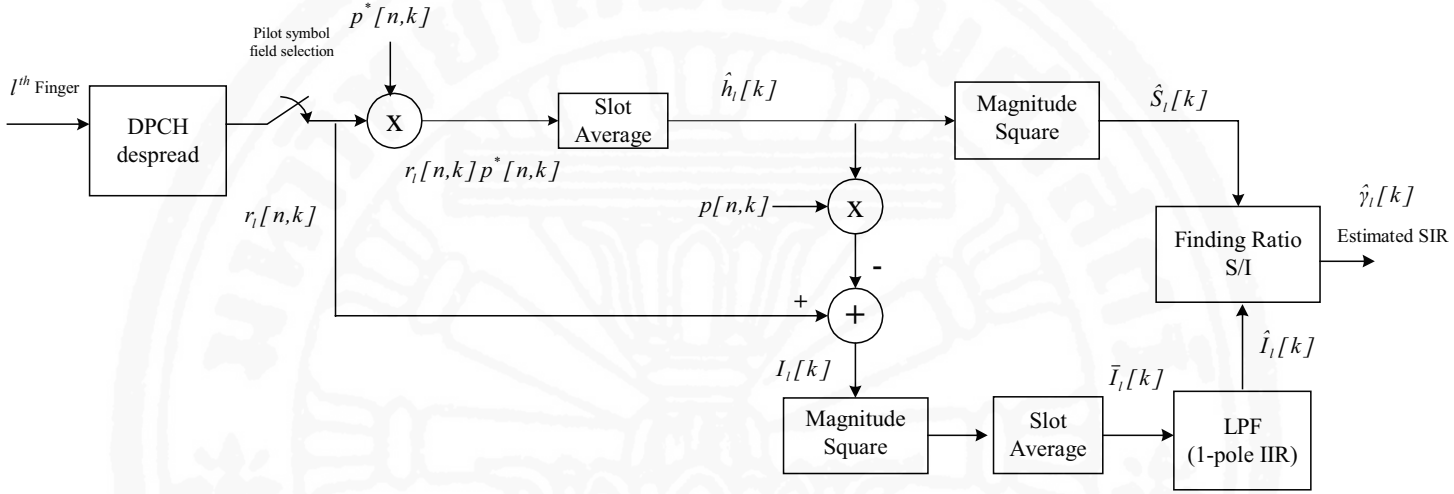

Figure 3.1 Conventional SIR Estimator

Next the received signal is duplicated and separated into two ways, one is used for calculating the power of the signal in terms of channel impulse response, and the other is used for calculating the power of the interference. Since the pilot sequence is a complex signal; to find the power of the signal then the channel impulse response is found by multiplying the complex conjugate of that pilot sequence with the received signal and the estimated impulse response from l^{th} path in k^{th} slot can be expressed as

$$\begin{aligned} \hat{h}_l[k] &= \frac{1}{N_p}\sum_{n\in T_p} r_l[n,k]p^*[n,k], \\ &= h_l[k] + \frac{1}{N_p} z_l[k], \end{aligned} \tag{3.2}$$

where N_p is the number of symbols in T_p and T_p is the field of the pilot symbol in DPCH sequence.

Therefore, by taking magnitude square, the signal power $\hat{S}_l[k]$ of the k^{th} slot in the l^{th} path can be represented as

$$\hat{S}_l[k] = |\hat{h}_l[k]|^2. \tag{3.3}$$

On the other hand, after the estimated channel impulse response $\hat{h}_l[k]$ was found, then the estimated channel gain $\hat{h}_l[k]p[n,k]$, the pilot sequence at n^{th} symbol in k^{th} slot multiplied with this estimated channel impulse response, to estimate the instantaneous interference in k^{th} slot from l^{th} path by subtracting the estimated channel gain from the received signal $r_l[n,k]$ as follows

$$I_l[k] = r_l[n,k] - \hat{h}_l[k]p[n,k]. \tag{3.4}$$

By taking magnitude square, then the interference power $\overline{I}_l[k]$ in k^{th} slot can be expressed as

$$\overline{I}_l[k] = \frac{1}{N_p}\sum_{n\in T_p} |I_l[k]|^2, \tag{3.5}$$

$$= \frac{1}{N_p}\sum_{n\in T_p} |r_l[n,k] - \hat{h}_l[k]p[n,k]|^2. \tag{3.6}$$

To cancel any unexpected noises, 1-pole IIR filter which is low pass characteristic is used at the final stage, therefore the output of the low pass filter can be shown as

$$\hat{I}_l[k] = \alpha\hat{I}_l[k-1] + (1-\alpha)\hat{I}_l[k], \tag{3.7}$$

where α is the pole of the IIR filter. Finally, the power ratio between signal and interference can be written as

$$\hat{\gamma}_l[k] = \frac{\hat{S}_l[k]}{\hat{I}_l[k]}. \tag{3.8}$$

3.1.2 Adjustable SIR Estimator

When the channel has slow multipath fading, there is strong correlation between the signals in the adjacent slots. As a result, it may be possible to obtain an improved SIR estimate by considering the signals in the adjacent slots. Since the channel condition is time varying, it is desirable to a adjust the number of slots for SIR estimation in response to the channel condition.

The adjustable SIR estimate scheme, as shown in Figure 3.2, considers the use of previous $\hat{h}_l[k]$ depending on the channel condition parameters obtained by the channel condition estimator. To optimally combine the precious channel gains, it may be desirable to employ a low pass filter whose coefficients are adjustable according to the channel condition. For ease of design, the moving average (MA) filter whose tap size N is adjusted depending upon the channel condition is considered. The estimate of the channel impulse response in k^{th} slot can be calculated by

$$\begin{aligned}
\overline{h}_{l,N}[k] &= \frac{1}{N}\sum_{j=1}^{N}\hat{h}_l[k-(j-1)], \\
&= \frac{1}{N}\frac{1}{N_p}\sum_{j=1}^{N}\sum_{n\in T_p}\{\hat{h}_l[n,k-(j-1)]+z_l[n,k-(j-1)]\}, \\
&= h_l[k]+\frac{1}{N}\frac{1}{N_p}z_l[k], \qquad (3.9)
\end{aligned}$$

where N is the tap size of the MA filter. Then, the signal power is estimated as

$$\hat{S}_l[k] = |\hat{h}_{l,N}[k]|^2. \qquad (3.10)$$

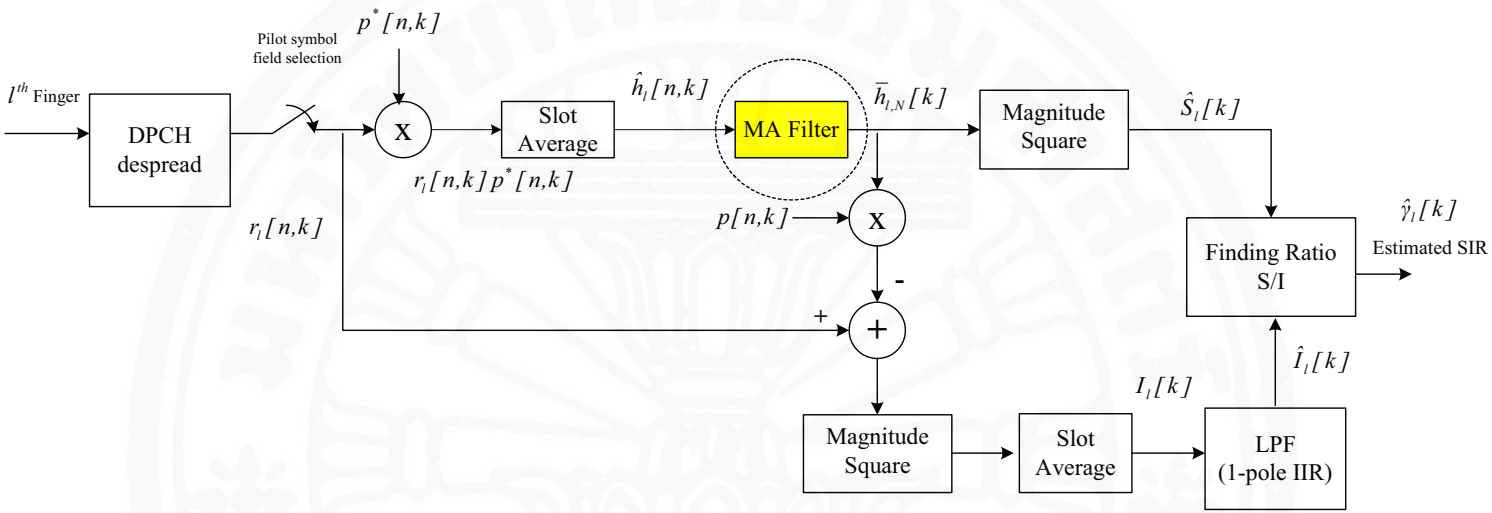

Figure 3.2 Adjustable SIR Estimator

And the instantaneous interference of the k^{th} slot can be represented by

$$I_l[k] = \frac{1}{N_p} \sum_{n \in T_p} |r_l[n,k] - \overline{h}_{l,N}[k]p[n,k]|^2. \tag{3.11}$$

3.2 Improving Performance with a Post-processing stage

A post-processing stage is applied for reducing the fluctuation of the estimated SIR with respect to the channel condition (Doppler frequency or equivalently the velocity of the mobile phone). From Figure 3.3, the received signal $r_l[n,k]$ is separated to the SIR estimator and velocity estimator. The algorithm of an adjustable SIR estimator is already shown in Figure 3.2 while the velocity estimator is used to estimate the Doppler frequency f_d and then sending it through the look up table to find the suitable value of tap size N for SIR estimator and suitable value of parameter(s) for the post-processing stage depending on the type of the filter. Since Table 3.1 shows the parameter(s) used for each filter.

In this thesis, four additional variations of the SIR are proposed and compared, namely
- SIR estimator with a moving average (MA) post-filter
- SIR estimator with an exponential moving average (EMA) post-filter
- SIR estimator with an IIR post-filter
- SIR estimator with least-mean-squared (LMS) adaptive post-filter

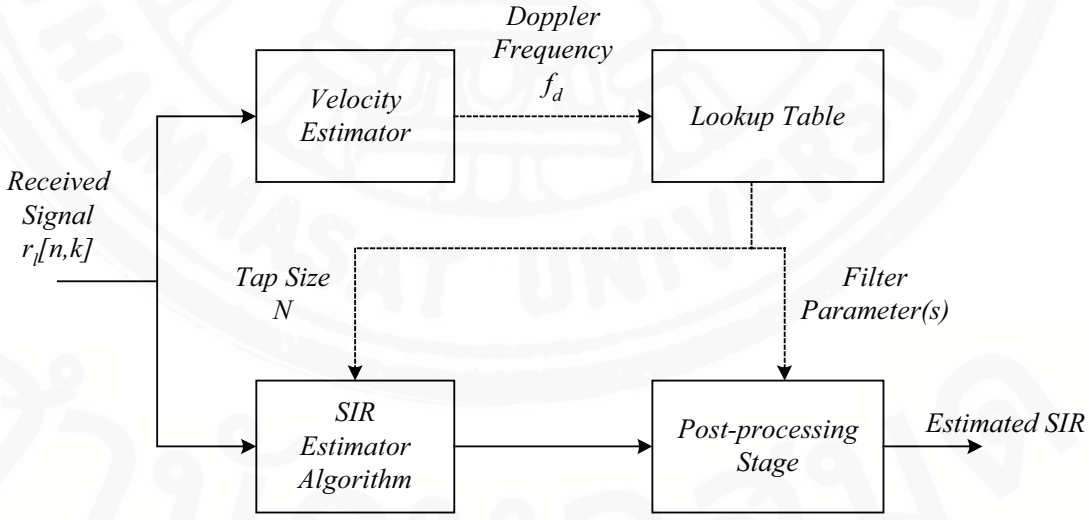

Figure 3.3 Post-Processing Scheme

Table 3.1 Parameter used in each filter

Type of filter	Parameter(s)
MA	window size (W)
EMA	weight parameter (w)
IIR	filter coefficients (order & cutoff frequency)
LMS	step size (μ)

3.2.1 Moving Average (MA) Filter

The block diagram of the MA filter is shown in Figure 3.4. This filter is the non-causal filter with odd window size W and makes use of the estimated SIR $\hat{\gamma}_l[k]$ according to the changing channel. Therefore, the new SIR of the l^{th} path can be estimated as

$$\overline{\gamma}_l[k] = \frac{1}{W} \sum_{k=i-\frac{W-1}{2}}^{k=i+\frac{W-1}{2}} \hat{\gamma}_l[k], \quad \forall i, \tag{3.12}$$

and

$$\overline{\gamma}_l[k] = \hat{\gamma}_l[k], \text{ for } k \leq \frac{W-1}{2}, \tag{3.13}$$

where k is the slot number, and W is the window size of the MA filter.

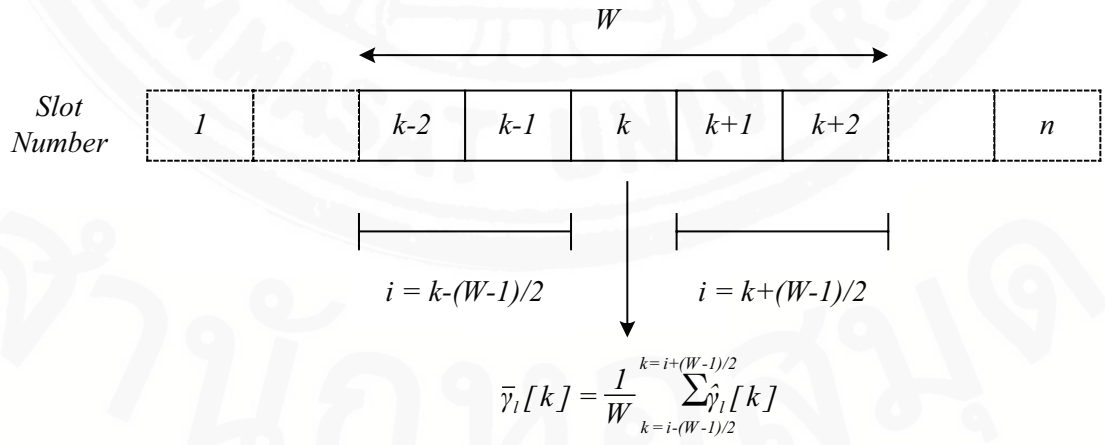

Figure 3.4 The Structure of MA Filter

3.2.2 Exponential Moving Average (EMA) Filter

The second way to improve the SIR values is apply an exponential moving average (EMA) filter instead the non-causal MA filter. The block diagram of this scheme is represented in Figure 3.5. and the new estimated SIR can be written as

$$\overline{\gamma}_l[k] = \beta\hat{\gamma}_l[k] + (1-\beta)\overline{\gamma}_l[k-1], \quad \text{for } k > 1, \tag{3.14}$$

and

$$\overline{\gamma}_l[k] = \hat{\gamma}_l[k], \text{ for } k = 1, \tag{3.15}$$

where $\beta = \frac{2}{w+1}$, and w is the weight parameter.

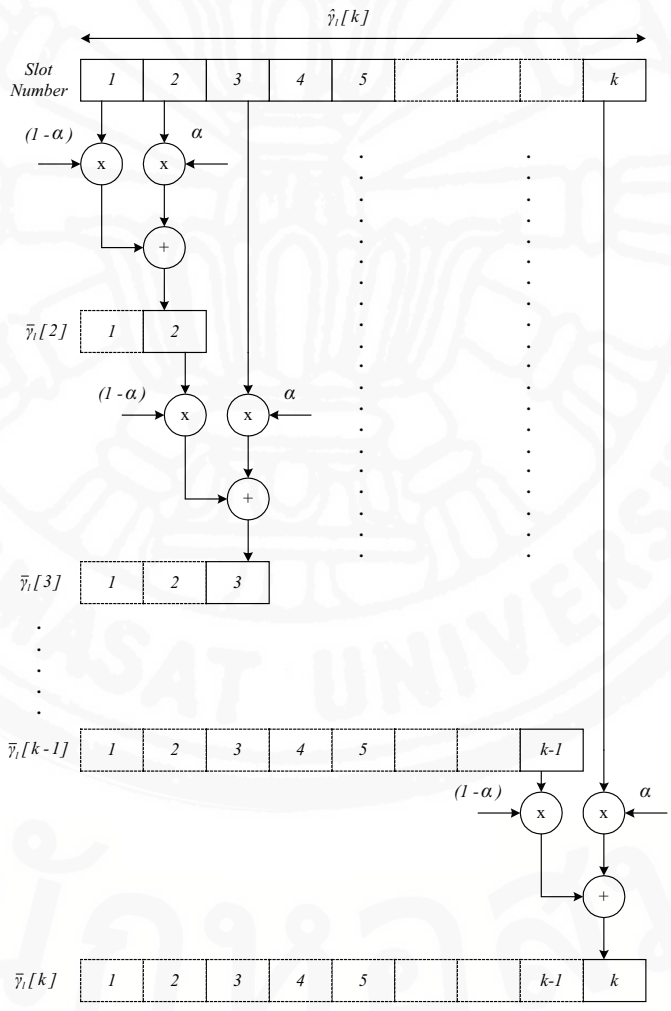

Figure 3.5 The Structure of EMA Filter

3.2.3 IIR Filters

Another way to improve the SIR values is makes use the IIR filter, in this thesis, three types of IIR filter namely, Chebyshev filter, and Butterworth filter are used at the post-processing stage instead those two algorithms presented above.

The transmission functions for Chebyshev filters of even and odd order are shown in Eq. 3.16-Eq. 3.17. The Chebyshev filter exhibits an equiripple response in the passband and a monotonically decreasing transmission in the stopband. While the odd-order filter has $|T(0)| = 1$, the even-order filter exhibits its maximum magnitude deviation at $\omega = 0$. In both cases the total number of passband maxima and minima equals the order of the filter, X. All the transmission zeros of the Chebyshev filter are at $\omega = \infty$, making it an all-pole filter.

The magnitude of the transfer function of an X^{th} order Chebyshev filter with a pass-band edge (ripple bandwidth) ω_p is given by

$$|T(j\omega)| = \frac{1}{\sqrt{1 + \epsilon^2 \cos^2[X \cos^{-1}(\omega/\omega_p)]}}, \text{ for } \omega \leq \omega_p, \tag{3.16}$$

and

$$|T(j\omega)| = \frac{1}{\sqrt{1 + \epsilon^2 \cosh^2[X \cosh^{-1}(\omega/\omega_p)]}}, \text{ for } \omega \geq \omega_p. \tag{3.17}$$

At the passband edge, $\omega = \omega_p$, the magnitude function is given by

$$|T(j\omega_p)| = \frac{1}{\sqrt{1 + \epsilon^2}}. \tag{3.18}$$

Thus, the parameter ϵ determines the passband ripple according to

$$A_{max} = 10 \log(1 + \epsilon^2), \tag{3.19}$$

Conversely, given A_{max}, the value of ϵ is determined from

$$\epsilon = \sqrt{10^{A_{max}/10} - 1}. \tag{3.20}$$

The attenuation achieved by the Chebyshev filter at the stopband edge $(\omega = \omega_s)$ is found using Eq. 3.17 as

$$A(\omega_s) = 10 \log[1 + \epsilon^2 \cosh^2(X \cosh^{-1}(\omega_s/\omega_p))]. \tag{3.21}$$

With the aid of a calculator this equation can be used to determine the order X required to obtain a specified A_{min} by finding the lowest integer value of X that yields $A(\omega_s) \geq A_{min}$.

As in the case of the Butterworth filter, increasing the order X of the Chebyshev filter causes its magnitude function to approach the ideal brick-wall low-pass response. And the poles of the Chebyshev filter are given by

$$\begin{aligned} p_k &= -\omega_p \sin(\frac{2k-1}{X}\frac{\pi}{2}) \sinh(\frac{1}{X}\sinh^{-1}\frac{1}{\epsilon}) + \\ & \quad j\omega_p \cos(\frac{2k-1}{X}\frac{\pi}{2}) \cosh(\frac{1}{X}\sinh^{-1}\frac{1}{\epsilon}), \end{aligned} \tag{3.22}$$

$$\text{for} \quad k = 1, 2, ..., X.$$

Therefore, the transfer function of the Chebyshev filter can be written as

$$T(s) = \frac{K\omega_p^X}{\epsilon 2^{X-1}(s-p_1)(s-p_2)...(s-p_X)}, \tag{3.23}$$

where K is the dc gain that the filter is required to have.

Next is the Butterworth filter, this filter exhibits a monotonically decreasing transmission with all the transmission zeros at $\omega = \infty$, making it an all-pole filter. The magnitude function for an X^{th} order Butterworth filter with a passband edge ω_p is given by

$$|T(j\omega)| = \frac{1}{\sqrt{1+\epsilon^2(\frac{\omega}{\omega_p})^{2X}}}. \tag{3.24}$$

At $\omega = \omega_p$

$$|T(j\omega_p)| = \frac{1}{\sqrt{1+\epsilon^2}}. \tag{3.25}$$

Thus the parameter ϵ determines the maximum variation in passband transmission, A_{max}, according to

$$A_{max} = 20\log\sqrt{1+\epsilon^2}, \tag{3.26}$$

Conversely, given A_{max}, the value of ϵ can be determined from

$$\epsilon = \sqrt{10^{A_{max}/10} - 1}. \tag{3.27}$$

Observe that in the Butterworth response the maximum deviation in passband transmission (from the ideal value of unity) occurs at the passband edge only. It can be shown that the first $2X-1$ derivatives of $|T|$ relative to ω are zero at $\omega = 0$. This property makes the Butterworth response very flat near $\omega = 0$ and gives the response the name maximally flat response. The degree of passband flatness increases as the order X is increased, and as the order X is increased the filter response approaches the ideal brick-wall type response.

At the edge of the stopband, $\omega = \omega_s$, the attenuation of the Butterworth filter is given by

$$A(\omega_s) = -20\log[1/\sqrt{1+\epsilon^2(\omega_s/\omega_p)^{2X}}], \quad (3.28)$$

$$= 10\log[1+\epsilon^2(\omega_s/\omega_p)^{2X}]. \quad (3.29)$$

This equation can be used to determine the filter order required, which is lowest integer value of X that yields $A(\omega_s) = A_{min}$.

Then, the transfer function can be written as

$$T(s) = \frac{K\omega_0^X}{(s-p_1)(s-p_2)...(s-p_X)}, \quad (3.30)$$

where K is also a constant equal to the required dc gain of the filter.

3.2.4 Least-Mean-Squared (LMS) Adaptive Filter

Adaptive filters are digital filters capable of self-adjustment. These filters can change in accordance to their input signals. It relies for its operation on a recursive algorithm which makes it possible for the filter to perform satisfactorily in environment where complete knowledge of the relevant signal characteristics is not available. According to these intelligent characteristics of the adaptive filter, the adaptive filter requires two inputs which are the input signal $x(n)$ and the desire signal $d(n)$.

Adaptive filters have the ability to update their coefficients. New coefficients are sent to the filter from a coefficient generator. The coefficient generator modifies the coefficient in response to the incoming signal.

As shown in Figure 3.6, the unknown system is modelled by an FIR filter with adjustable coefficients. Both the unknown system and the FIR filter are excited by an input signal $x(n)$. The adaptive filter output $y(n)$ is compared with desired response $d(n)$ to produce the error signal $e(n)$. The error signal represents the difference between the unknown system output and the model output. The error $e(n)$ is used as the input to the adaptive control algorithm, which corrects individual tap weight of the filter. This process is repeated through several iterations until the error signal $e(n)$ becomes sufficiently small.

The least-mean-squared (LMS) adaptive algorithm is a linear filtering algorithm that consists of two basic processes:

1. A Filtering Process: This process involves

(a) Computing the output of a linear filter in response to the input signal.

(b) Generating an estimation error by comparing this output with a desired response.

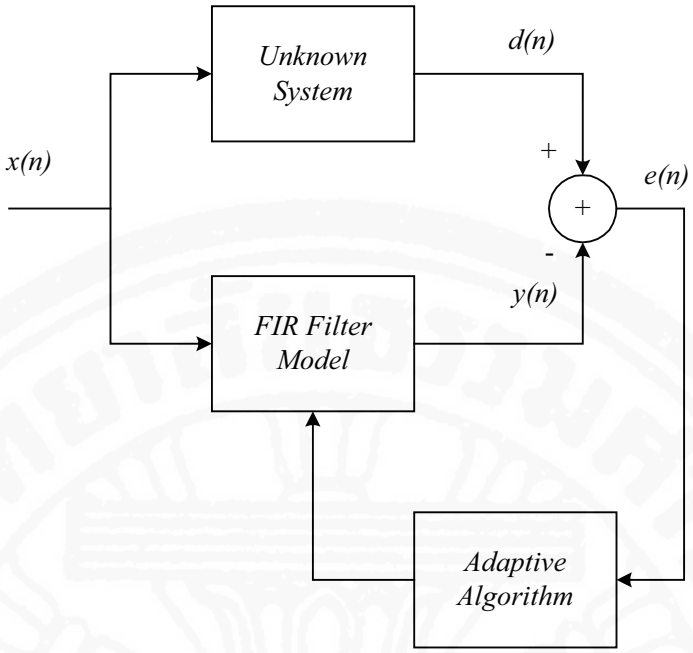

Figure 3.6 System identification model

2. An Adaptive Process: This process involves automatic adjustment of the parameters of the filter according to the estimation error.

The combination of these two processes constitutes a feedback loop, as illustrated in Figure 3.7. First, the LMS filter is built around a transverse filter; this component is responsible to the filtering process. Then, the mechanism for adaptive control of the tap weights of the transversal filter will be used.

Details of the transversal filter component are presented in Figure 3.8. The tap inputs $u(n), u(n-1), ..., u(n-M+1)$ form the elements of $(M - by - 1)$ tap-input vector $u(n)$, where $M-1$ is the number of delay elements. Correspondingly, the tap weights $\hat{w}_0(n), \hat{w}_1(n), ..., \hat{w}_{M-1}(n)$ form the elements of $(M - by - 1)$ tap-weight vector $\hat{\mathbf{w}}(n)$.

The value computed for this vector using an LMS algorithm represents an estimate whose expected value may come close to the Wiener solution $\mathbf{w}_0$, in wide-sense stationary environment, as the number of iterations n approaches to infinity.

During the filtering process, the desired response $d(n)$ is supplied for processing, alongside the tap-input vector $u(n)$. Given this input, the transversal filter produces an output $y(n)$ used as an estimate of the desired response $d(n)$. Accordingly, we may define as estimate error $e(n)$ as the difference between the desired response and the actual filter output, as indicated in the output at the end of Figure 3.8. The estimation error $e(n)$ and the tap-input vector $u(n)$ are applied to the control mechanism, and the feedback loop around

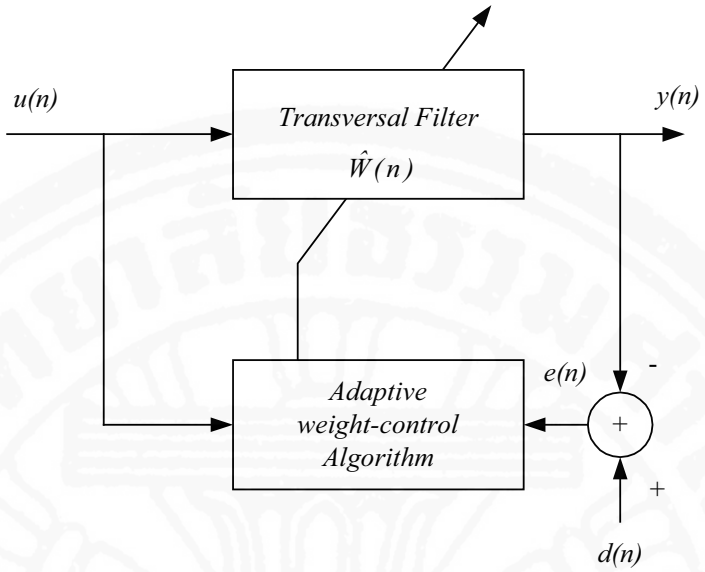

Figure 3.7 Block Diagram of Adaptive Transversal Filter

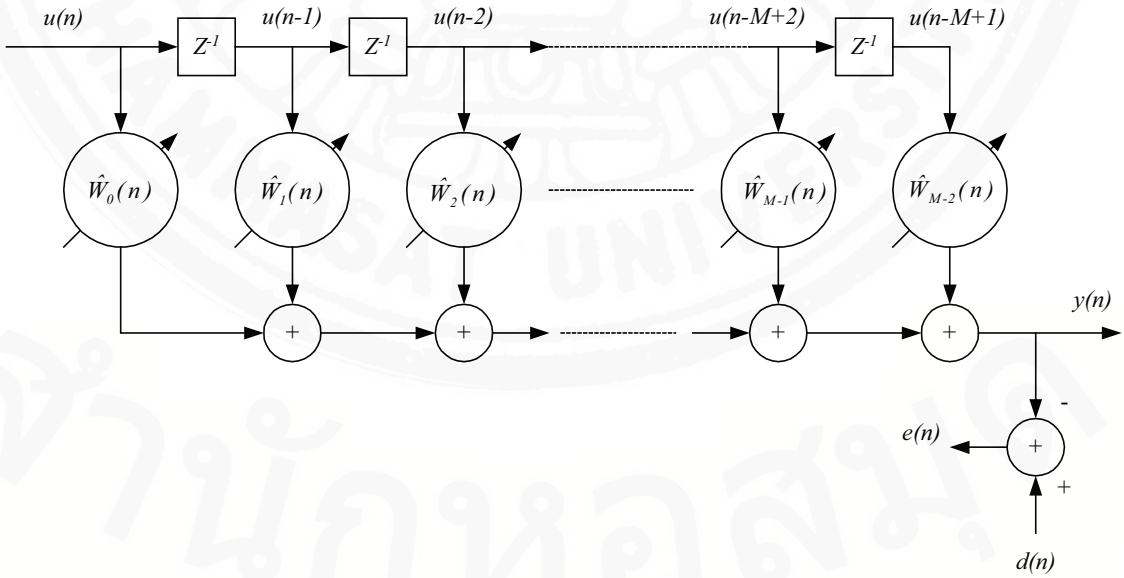

Figure 3.8 Detail Structure of the Transversal Filter Component

the tap weights is thereby close.

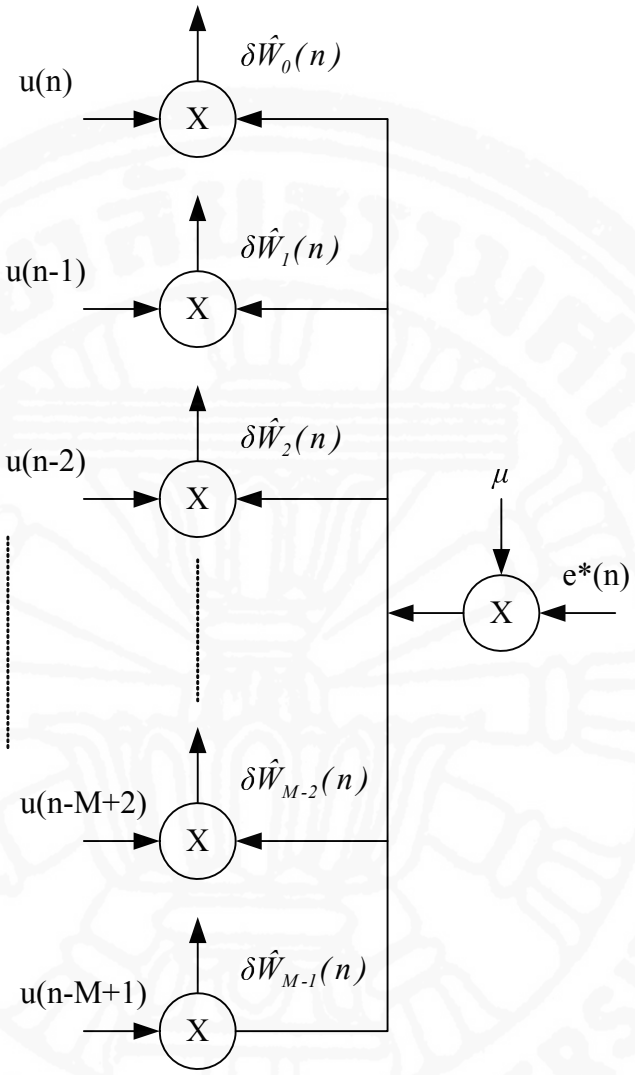

Figure 3.9 The Structure of the Adaptive Weight Control Mechanism

Figure 3.9 represents details of the adaptive weight-control mechanism. Specifically, a scalar version of the inner product of the estimation error $e(n)$ and the tap input $u(n-k)$ is computed for $k = 0, 1, 2, ..., M-2, M-1$. The obtained result defines the correction $\delta\hat{w}_k(n)$ applied to the tap weight $\hat{w}_k(n)$ at iteration $n+1$. The scaling factor used in this computation is denoted by a positive quantity μ in Figure 3.10 called the step-size parameter. To conserve the stability, an important criterion is required:

$$J(n) \rightarrow J(\infty) \text{ as } n \rightarrow \infty, \tag{3.31}$$

where $J(n)$ is the mean-square error produced by the LMS filter at time n and its final value $J(\infty)$ is a constant. An algorithm that satisfies this requirement is said to be stable in the mean square. For the LMS algorithm to satisfy this criterion, the step-size parameter μ has to satisfy a certain condition related to the spectral content of the tap inputs.

If the input vector $\mathbf{u}(n)$ and the design response $d(n)$ are jointly stationary, the cost function $J(n)$ at time n is written by using the definitions of the correlation matrix **R** and the cross-correlation vector **p** as

$$J(n) = \sigma^2 - w^H(n)\mathbf{p} - \mathbf{p}^H w(n) + w^H(n)\mathbf{R}w(n). \tag{3.32}$$

To develop an estimate of the gradient vector $\nabla J(n)$ at each iteration n, the most obvious strategy is to substitute estimates of the correlation matrix **R** and the cross-correlation vector **p**, can be expressed by

$$\nabla J(n) = -2\mathbf{p} + 2\mathbf{R}w(n). \tag{3.33}$$

Instantaneous estimates for **R** and **p** are the simplest choice of estimators, which are based on sample values of the tap-input vector and desired response, defined by

$$\hat{\mathbf{R}}(n) \;=\; \mathbf{u}(n)\mathbf{u}^H(n), \tag{3.34}$$

and

$$\hat{\mathbf{p}}(n) \;=\; \mathbf{u}(n)d^*(n). \tag{3.35}$$

An exact estimate of the gradient vector $\nabla J(n)$ at each iteration n and suitable step-size parameter μ are needed in computing optimum tap-weight vector, $\hat{\mathbf{w}}(n)$. Therefore, the instantaneous estimate of the gradient vector is

$$\hat{\nabla} J(n) = -2\mathbf{u}(n)d^*(n) + 2\mathbf{u}(n)\mathbf{u}^H(n)\hat{\mathbf{w}}(n). \tag{3.36}$$

However, this estimate is biased, because the tap-weight estimate vector $\hat{\mathbf{w}}(n)$ depends on the tap-input vector $\mathbf{u}(n)$.

Therefore, the result in the form of three basic relations can be expressed as follows:

1. Filter output:

$$y(n) = \hat{\mathbf{w}}^H(n)\mathbf{u}(n). \tag{3.37}$$

2. Estimation error or error signal:

$$e(n) = d(n) - y(n). \tag{3.38}$$

3. Tap-weight adaptation:

$$\hat{\mathbf{w}}(n+1) = \hat{\mathbf{w}}(n) + \mu \mathbf{u}(n) e^*(n). \tag{3.39}$$

Eq. 3.37 and Eq. 3.38 define the computation of the estimation error $e(n)$ which is based on the current estimate of tap-weight vector $\hat{w}(n)$. The term $\mu \mathbf{u}(n) e^*(n)$ is considered as the adjustment that is applied to $\hat{w}(n)$, where its initial condition is set to be $\hat{w}(0)$. The algorithm described by Eq. 3.37-Eq. 3.39 is the complex form of the adaptive LMS algorithm. The knowledge of the most recent values (e.g. $u(n), d(n)$, and $\hat{w}(n)$) is required for this algorithm at each time update. A signal-flow graph representation of the LMS algorithm in the form of feedback model shown in Figure 3.10, where the simplicity of the LMS algorithm is illustrated. From Figure 3.10, the LMS algorithm requires only $2M + 1$ complex multiplications and $2M$ complex additions per iteration. M is the number of tap weights used in the adaptive transversal filter. Since the instantaneous estimates of **R** and **p** are used in the algorithm, the LMS algorithm seems to be incapable of performing well at first sight. During the course of adaption, these estimate is averaged effectively because LMS algortihm is recursive in nature.

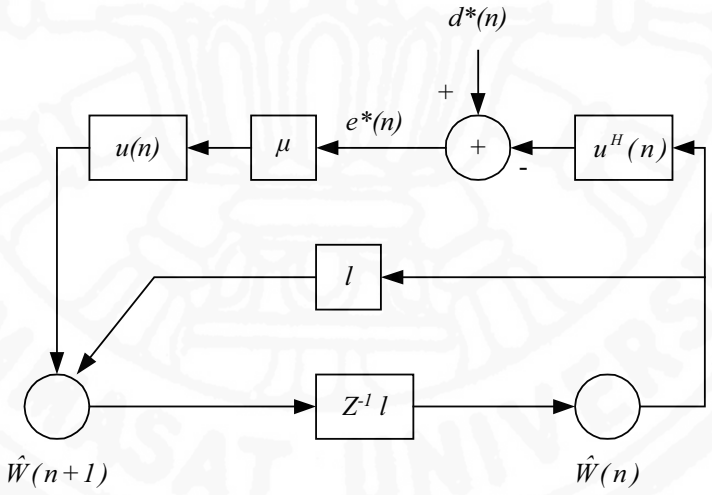

Figure 3.10 Signal flow graph representation of LMS algorithm

3.3 Performance Comparison of SIR Estimators

In this thesis, the performance of all schemes are evaluated by using computer simulation with the following input parameters shown in Table 3.2. And the performance of the new SIR estimator is measured in terms of root-mean-square error (RMSE).

Table 3.2 Input Parameters

Pilot bits per Slot (N_p)	4
Doppler Frequency (f_d)	0-250 Hz
Channel Model	ITU Vehicular B
AWGN	-12dB

The channel is assumed to have only one path signal for simplicity of simulation. The performance of the three SIR estimate schemes, namely, the conventional SIR estimator, the adjustable (adaptive) SIR estimator, and the SIR estimator with post-processing scheme are depicted in Figure 3.11.

The reason of showing Figure 3.11 because we need to show that the adjustable SIR estimator with post-processing stage can improve the performance of the system.

Since the time-varying characteristics of the channel is mostly effected by the Doppler frequency which directly related to the speed as described in Eq. 3.40 as follow

$$f_d = v f_c / c, \tag{3.40}$$

where f_d is the Doppler frequency, f_c is the carrier frequency, c and v are the speed of the light and the mobile, respectively.

From Figure 3.12, it is also proved that the adjustable SIR estimator with post-processing scheme give the better performance than the normal scheme.

Figure 3.13 shows the performance comparison between IIR post-filtering and EMA post-filtering.

In this simulations, after using MATLAB program, the suitable window size W for MA filter, the optimal weight parameter w for EMA filter, the filter coefficients for IIR filter, and the step-size parameter μ for LMS adaptive algorithm are found by searching and minimizing the mean-square-error (MSE).

In case of IIR filter, the ripple is considered at 0.1dB. While LMS algorithm, LMS adaptive filter operates on an input vector $\mathbf{u}(n)$ and the desired response $d(n)$ to produce a minimum mean-square error, which is adjustable by varying the filter length M. From trial and error method, the filter length is chosen to be $M = 12$. To demonstrate the SIR estimation, the LMS adaptive filter coefficient (e.g. Tap-weight, w) is updated until the optimal value that provides the minimum RMSE is obtained. The step-size parameter μ is suitably chosen to obtain the optimum tap-weight vector.

Figure 3.14 displays the performance of the SIR estimation scheme, namely (a) the adjustable (adaptive) estimation scheme and (b) LMS adaptive estimation scheme over 1500

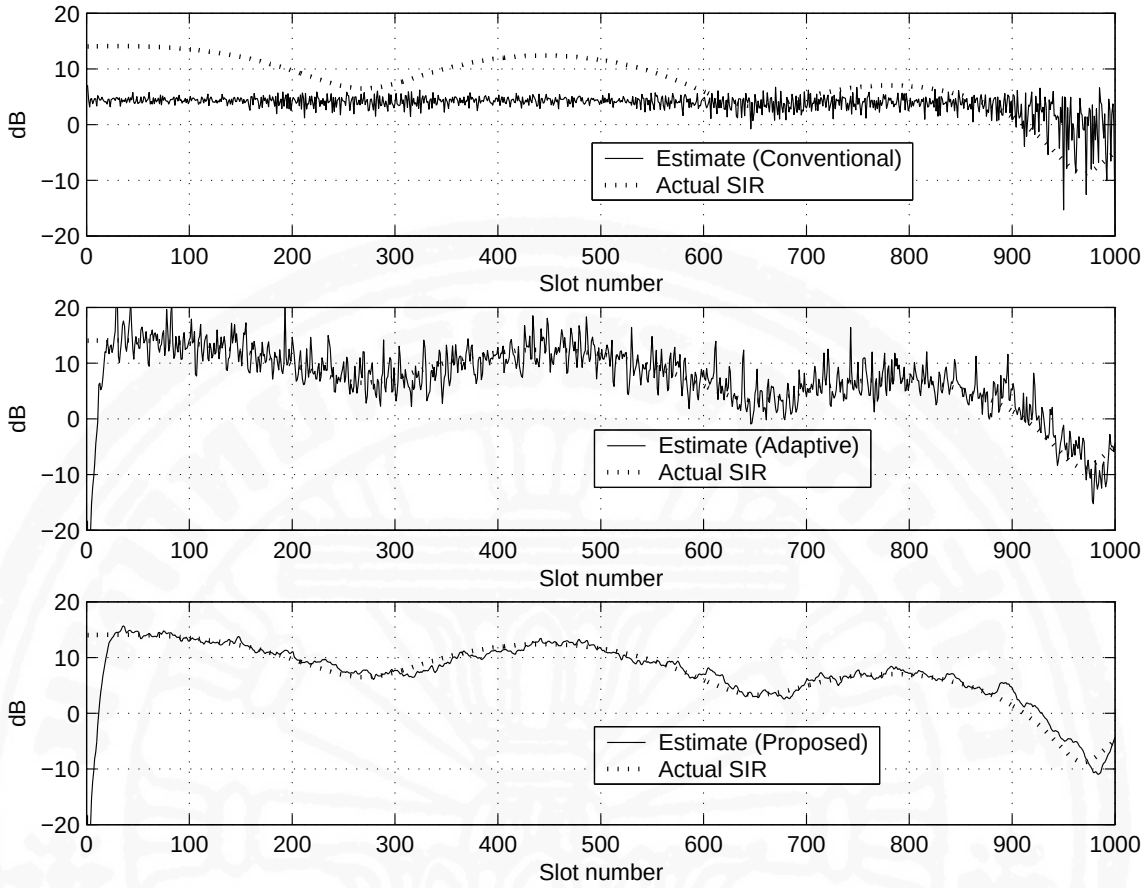

Figure 3.11 The plots of estimated SIR vs the actual SIR using (top) conventional scheme, (middle) adjustable (adaptive) scheme and (bottom) adjustable (adaptive) scheme with MA post-filtering

slot numbers under interference and noise, viewed cumulatively as additive white Gaussian noise, is generated at -12dB.

In real environment where the complete knowledge of characteristics of the desired signal is not available, the delay of the input vector $\mathbf{u}(n-1)$ is replaced and used in the computation of the estimation error $\mathbf{e}(n)$ by comparing to the output $\mathbf{y}(n)$. Table 3.8 displays μ values corresponding to the RMSE at different Doppler frequency and the suitable step-size parameter is chosen to be 0.0000062. After getting the optimal tap-weight, the SIR estimation is obtained through direct calculation. The performances of SIR estimate are displayed in Figure 3.14. The obtained SIR estimation of both LMS adaptive schemes provide large fluctuation over the first 500 slot numbers. This is a result of the tap-weight adaptation where the convergence time is needed to converges to an optimal value since the tap-weight vector, at first, was set to be zero. The final result is the smoother SIR estimated at the long number of iterations.

For the actual implementation of the lookup table, Table 3.3 summarizes the effect of

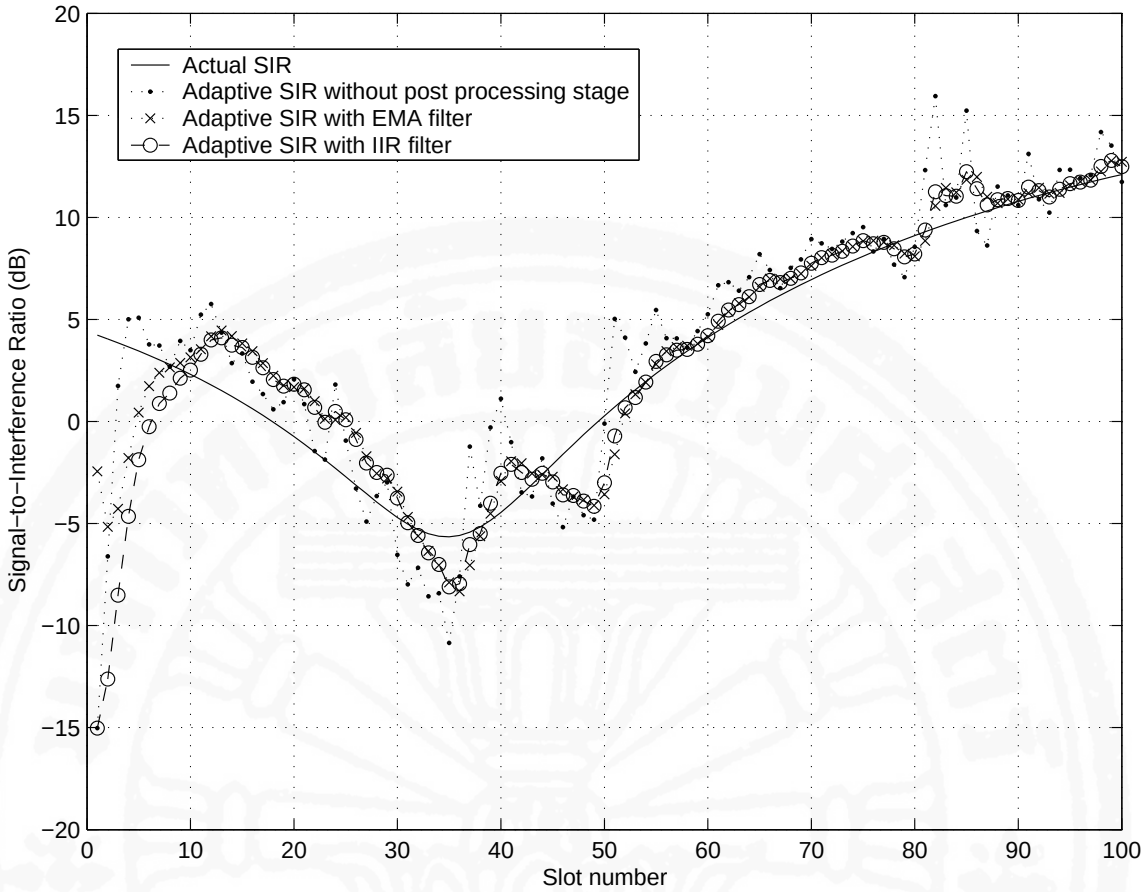

Figure 3.12 Signal-to-Interference Ratio vs slot number for Doppler frequency $f_d = 10Hz$ and tap size $N = 4$

the Doppler frequency on the tap size of the first MA filter in the adjustable SIR estimator, and the sub-optimal window size, W, used in the second MA filter at the post-processing stage, Table 3.4 summarizes about the effect of the Doppler frequency on the weight parameter, w, Table 3.5-3.7 summarize the effect of the Doppler frequency on the filter coefficients of each IIR filter, and Table 3.8 summarizes the effect of the Doppler frequency on the step-size parameter, μ.

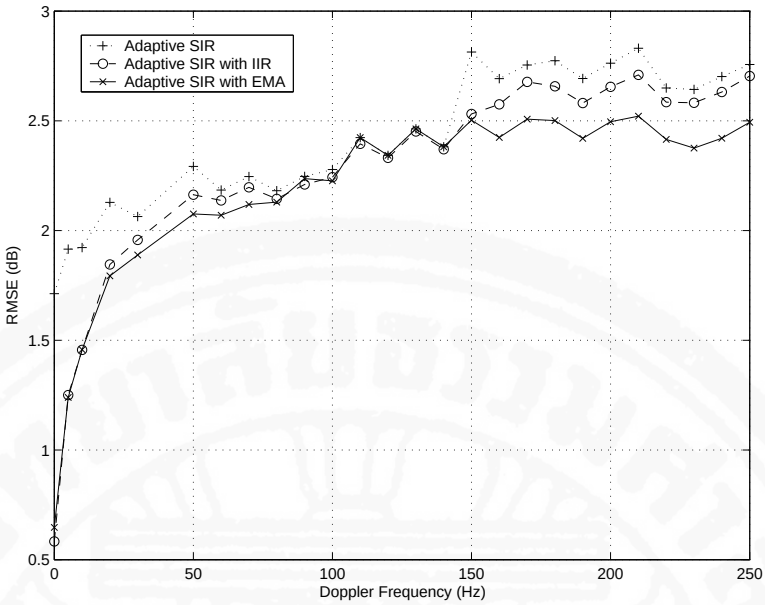

Figure 3.13 RMSE vs f_d of an Adjustable (adaptive) SIR with and without post-processing stage

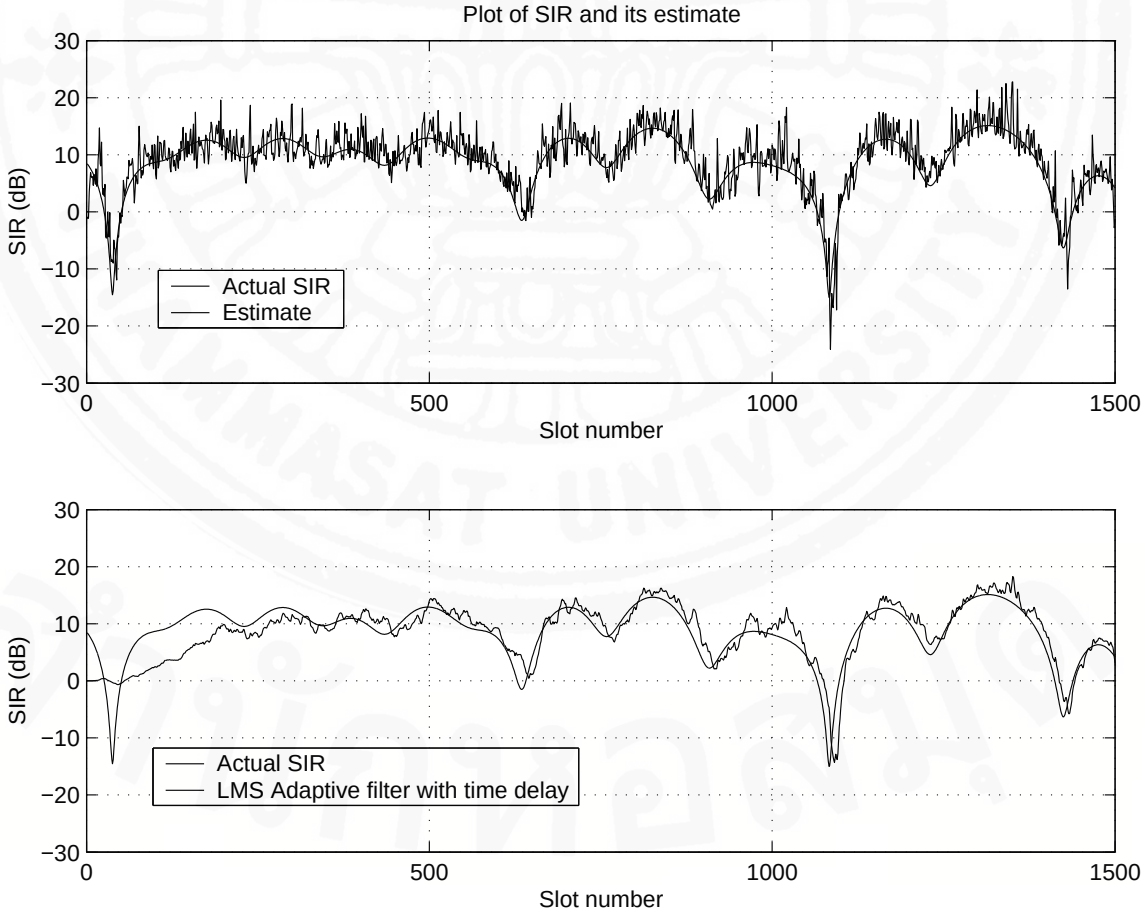

Figure 3.14 (a) Adjustable (adaptive) SIR estimator, (b) LMS Adaptive estimator

Table 3.3 Lookup Table for MA Filter

Doppler Frequency (f_d)	Optimal Tap Size (N)	Optimal Window Size (W)	Minimum RMSE (dB)
0	20	159	0.8437
5	20	61	1.1060
10	8	45	1.2340
20	8	27	1.3140
30	6	17	1.6748
50	5	15	1.7841
60	5	15	1.6843
70	4	11	1.8218
80	4	9	1.9344
90	4	11	1.9611
100	3	9	2.1012
110	3	9	1.9593
120	3	9	2.0234
130	3	7	2.1232
140	3	7	1.9945
150	3	7	2.1237
160	3	7	2.1991
170	3	7	2.2795
180	3	7	2.2048
190	3	7	2.4185
200	3	5	2.4668
210	2	5	2.4722
220	3	7	2.4166
230	2	5	2.5269
240	2	5	2.3558
250	2	5	2.4749

Table 3.4 Lookup Table for EMA Filter

Doppler Frequency (f_d)	Optimal Tap Size (N)	Optimal Weight Parameter (w)	Minimum RMSE (dB)
0	7	39	1.480
5	6	12	3.046
10	6	13	3.175
20	4	7	4.882
30	5	5	4.626
50	4	4	6.067
60	4	5	5.718
70	3	4	6.977
80	3	3	7.387
90	3	3	7.465
100	3	3	7.030
110	3	3	7.901
120	3	3	8.176
130	3	2	9.065
140	3	2	8.777
150	3	2	8.437
160	3	2	8.863
170	2	2	8.872
180	2	2	9.095
190	2	2	9.531
200	2	2	9.540
210	2	2	9.944
220	2	2	9.277
230	2	2	9.389
240	2	2	10.500
250	2	2	9.988

Table 3.5 Lookup Table for Chebyshev Filter Type I

Doppler Frequency (f_d)	Optimal Tap Size (N)	Order (X)	Normalized Cut-Off Frequency	Minimum RMSE (dB)
0	18	1	0.002	0.585
50	2	1	0.072	2.163
100	2	2	0.9	2.243
150	2	1	0.9	2.532

Table 3.6 Lookup Table for Chebyshev Filter Type II

Doppler Frequency (f_d)	Optimal Tap Size (N)	Order (X)	Normalized Cut-Off Frequency	Minimum RMSE (dB)
0	18	1	0.002	0.585
50	2	1	0.072	2.163
100	2	2	0.4	2.266
150	2	2	0.9	2.531

Table 3.7 Lookup Table for Butterworth Filter

Doppler Frequency (f_d)	Optimal Tap Size (N)	Order (X)	Normalized Cut-Off Frequency	Minimum RMSE (dB)
0	18	1	0.011	0.583
50	2	1	0.409	2.163
100	2	1	0.9	2.280
150	2	1	0.9	2.539

Table 3.8 Lookup Table for LMS Adaptive Filter

Doppler Frequency (f_d)	Optimal Tap Size (N)	Optimal Step Size (μ)	Minimum RMSE (dB)
0	20	0.00000620	1.4146
30	20	0.00001405	2.3370
50	5	0.00001560	2.7200
60	5	0.00001310	2.6297
70	4	0.00001900	2.9180
80	4	0.00002215	3.0217
90	4	0.00001920	3.0350
100	3	0.00001910	2.9700
110	3	0.00002080	3.1620
120	3	0.00001820	3.1944
130	3	0.00002010	3.4236
140	3	0.00002000	3.4415
150	3	0.00002450	3.3461
160	3	0.00002030	3.4546
170	3	0.00002040	3.6976
180	3	0.00002070	3.8390
190	3	0.00002000	3.8602
200	3	0.00001510	3.5952
210	2	0.00001300	3.6856
220	3	0.00001800	4.1402
230	2	0.00001500	3.6515
240	2	0.00001200	3.3935
250	2	0.00001090	3.8625